

# Approximate Reachability Computation for Polynomial Systems

Thao Dang

VERIMAG, Centre Equation, 2 avenue de Vignate,  
38610 Gières, France  
Thao.Dang@imag.fr

**Abstract.** In this paper we propose an algorithm for approximating the reachable sets of systems defined by polynomial differential equations. Such systems can be used to model a variety of physical phenomena. We first derive an integration scheme that approximates the state reachable in one time step by applying some polynomial map to the current state. In order to use this scheme to compute all the states reachable by the system starting from some initial set, we then consider the problem of computing the image of a set by a multivariate polynomial. We propose a method to do so using the Bézier control net of the polynomial map and the blossoming technique to compute this control net. We also prove that our overall method is of order 2. In addition, we have successfully applied our reachability algorithm to two models of a biological system.

## 1 Introduction

Reachability analysis is an important problem in formal verification of hybrid systems. A major ingredient in designing a reachability analysis algorithm for hybrid systems is an efficient method to handle their continuous dynamics described by differential equations (since their discrete dynamics can be handled using existing discrete verification methods). Reachability computation methods for a special class of systems with constant derivatives are well-developed. On the other hand, while many well-known properties of linear differential equations can be exploited to design relatively efficient methods, non-linear systems are much more difficult to analyze. Numerical integration is a common method to solve non-linear differential equations. Its goal is to derive a scheme to approximate the solution at each time step based on the solution at one or several previous steps. In general, a typical numerical integration scheme can be written as:  $\mathbf{x}_{k+1} = \mathcal{Y}_k(f, h, \mathbf{x}_0, \mathbf{x}_1, \dots, \mathbf{x}_k)$  where  $f$  is the derivative and  $h$  is the step size. Nevertheless, while this approach is concerned with computing a single solution at a time and each  $\mathbf{x}_k$  in this scheme is a point, in reachability analysis one has to deal with sets of all possible solutions (due to non-determinism in initial conditions and in the dynamics of the system). Therefore, wishing to exploit the numerical integration idea for reachable set computation purposes, a question that arises is how to perform such schemes with sets, that is, when each  $\mathbf{x}_k$  is a set of points. The essence behind the approach we propose in this paper can be

described as extending traditional numerical integration to set integration. In particular, we are interested in systems defined by polynomial differential equations. Such systems can be used to model a variety of physical phenomena, in particular the dynamics of bio-chemical networks. We first derive an integration scheme that approximates the reachable state  $\mathbf{x}_{k+1}$  by applying some polynomial map to  $\mathbf{x}_k$ . In order to use this scheme to approximate the reachable set, we then consider the problem of computing the image of a set by a multivariate polynomial. To do so, we employ the techniques from computer aided geometric design, in particular the Bézier techniques and the blossoming principle. We also prove that our overall method is of order 2. Although this paper focuses on continuous systems, the proposed method can be extended to hybrid systems, since reachable sets are represented by convex polyhedra, and Boolean operations (required to deal with discrete transitions) over such polyhedra can be computed using a variety of existing algorithms. This is illustrated through an example in Section 3.

Before continuing, we present a brief review of related work. The reachability problem for continuous systems described by differential equations has motivated much research both for theoretical problems, such as computability (see for example [1]), and for the development of computation methods and tools. If the goal is to exactly compute the reachable set or approximate it as accurately as possible, one can use a variety of methods for tracking the evolution of the reachable set under the continuous flows using some set representation (such as polyhedra, ellipsoids, level sets) [2, 3, 4, 5, 6, 7, 8, 9]. Since high quality approximations are hard to compute, other methods seek approximations that are sufficiently good to prove the property of interest<sup>1</sup> (such as barrier certificates [10], polynomial invariants [11]). Abstraction methods for hybrid systems are also close in spirit to these methods. Indeed, their main idea is to approximate the original system with a simpler system (that one can handle more efficiently) and refine it if the analysis result obtained for the approximate system is too conservative (see for example [12, 13, 14, 15, 16]).

The paper is organized as follows. In Section 2, after stating our problem, we describe an integration scheme for polynomial differential equations. This scheme requires computing the image of a set by a polynomial map, the problem we discuss in Section 3. We then present our reachability algorithm and some experimental results obtained using the algorithm on the models of gene transcription control of the bacteria *Vibrio Fisherii*.

## 2 Reachability Analysis of Polynomial Systems

Throughout the paper, vectors are often written using bold letters. Given a vector  $\mathbf{x}$ ,  $\mathbf{x}[i]$  denotes its  $i^{\text{th}}$  component.

We consider a polynomial system:

$$\dot{\mathbf{x}}(t) = g(\mathbf{x}(t)). \quad (1)$$

---

<sup>1</sup> It should be noted that reachable set computations can also be used for controller synthesis where the accuracy criterion is important.

We first rewrite the dynamics of the system as the sum of its linear part  $A\mathbf{x}(t)$  and its non-linear part  $f(\mathbf{x}(t))$ , that is,

$$\dot{\mathbf{x}}(t) = g(\mathbf{x}(t)) = A\mathbf{x}(t) + f(\mathbf{x}(t)). \quad (2)$$

We then consider the non-linear term as independent input. In other words, the system is treated as a linear system with input  $f(\mathbf{x}(t))$ . This trick is to separate the linear part for which we can derive the exact closed-form solution. The interest in doing so will become clearer when we discuss the approximation error. We now develop a numerical solution for (2). Let  $h > 0$  be a time step and  $t_k = kh$  where  $k = 0, 1, 2, \dots$ . Then, we have

$$\mathbf{x}(t_{k+1}) = e^{Ah}\mathbf{x}(t_k) + \int_0^h e^{A(h-\tau)} f(\mathbf{x}(t_k + \tau)) d\tau. \quad (3)$$

The idea is to approximate  $\mathbf{x}(t_k + \tau)$  inside the above integral by its Taylor expansion around  $t_k$  to the first order, that is  $\boldsymbol{\alpha}(t_k + \tau) = \mathbf{x}(t_k) + g(\mathbf{x}(t_k))\tau$ . Denoting  $\mathbf{x}(t_k) = \mathbf{x}_k$ ,  $f(\mathbf{x}(t_k)) = f_k$  and  $g(\mathbf{x}(t_k)) = g_k$ , we have  $\boldsymbol{\alpha}(t_k + \tau) = \mathbf{x}_k + g_k\tau = \mathbf{x}_k + (Ax_k + f_k)\tau$ . Replacing  $\mathbf{x}(t_k + \tau)$  with  $\boldsymbol{\alpha}(t_k + \tau)$ , we obtain an approximation  $\bar{\mathbf{x}}_{k+1}$  of the exact solution  $\mathbf{x}_{k+1}$ :

$$\bar{\mathbf{x}}_{k+1} = e^{Ah}\mathbf{x}_k + \int_0^h e^{A(h-\tau)} f(\boldsymbol{\alpha}(t_k + \tau)) d\tau. \quad (4)$$

The integral in the above equation is a function of  $\mathbf{x}_k$ , and we denote it by  $Q(\mathbf{x}_k) = \int_0^h e^{A(h-\tau)} f(\boldsymbol{\alpha}(t_k + \tau)) d\tau$ .

**Proposition 1.** *The map  $Q(\mathbf{x}_k)$  can be written as a polynomial in  $\mathbf{x}_k$ .*

*Proof.* The proof of the proposition is straightforward, however we present it here for the clarity of the development that follows. It is easy to see that if the total degree of  $f(\mathbf{x})$  is  $d$  in  $\mathbf{x}$ , then  $\boldsymbol{\alpha}(t_k + \tau)$  is a multivariate polynomial of total degree  $d$  in  $\mathbf{x}_k$ , and therefore  $f(\boldsymbol{\alpha}(t_k + \tau))$  is a polynomial of degree  $d$  in  $\tau$ . We can write  $f(\boldsymbol{\alpha}(t_k + \tau)) = \sum_{l=0}^d \psi_l(\mathbf{x}_k)\tau^l$  where for every  $l \in \{0, 1, \dots, d\}$ ,  $\psi_l(\mathbf{x}_k)$  is a polynomial in  $\mathbf{x}_k$ . We then denote  $\Gamma_l = \int_0^h e^{A(h-\tau)}\tau^l d\tau$ , which can be written in a closed form. It then follows that  $\int_0^h e^{A(h-\tau)} f(\boldsymbol{\alpha}(t_k + \tau)) d\tau = \sum_{l=0}^d \Gamma_l \psi_l(\mathbf{x}_k)$ .  $\square$

The resulting integration scheme to approximate the solution of (1) is:

$$\begin{cases} \bar{\mathbf{x}}_{k+1} = e^{Ah}\bar{\mathbf{x}}_k + Q(\bar{\mathbf{x}}_k) = P(\bar{\mathbf{x}}_k), \\ \bar{\mathbf{x}}_0 = \mathbf{x}(0). \end{cases}$$

We call  $P(\mathbf{x}_k)$  the *integration map*.

**Example of multi-affine systems.** Let us illustrate the proof with a simple case where  $g(\mathbf{x})$  is a multi-affine function of degree 2. This is the case of a biological model we study in Section 5. The function  $f(\mathbf{x})$  can be written as:

$f(\mathbf{x}) = \sum_{i,j \in \{1, \dots, n\}, i \neq j} \mathbf{x}[i]\mathbf{x}[j]\mathbf{c}_{ij}$  with  $\mathbf{c}_{ij} \in \mathbb{R}^n$ . Then, replacing  $\mathbf{x}(t_k + \tau)$  with  $\alpha(t_k + \tau) = \mathbf{x}_k + g_k\tau$ , we have:

$$f(\alpha(t_k + \tau)) = \sum_{i \neq j \in \{1, \dots, n\}} (g_k[i]g_k[j]\tau^2 + (\mathbf{x}_k[i]g_k[j] + g_k[i]\mathbf{x}_k[j])\tau + \mathbf{x}_k[i]\mathbf{x}_k[j])\mathbf{c}_{ij}$$

Therefore, the equation (4) becomes:

$$\bar{\mathbf{x}}_{k+1} = P(\mathbf{x}_k) = \Phi\mathbf{x}_k + \sum_{i \neq j \in \{1, \dots, n\}} (\gamma_2\Gamma_2 + \gamma_1\Gamma_1 + \gamma_0\Gamma_0)\mathbf{c}_{ij}. \tag{5}$$

where  $\Phi = e^{Ah}$  and  $\gamma_2 = g_k[i]g_k[j]$ ,  $\gamma_1 = g_k[i]\mathbf{x}_k[j] + \mathbf{x}_k[i]g_k[j]$ ,  $\gamma_0 = \mathbf{x}_k[i]\mathbf{x}_k[j]$ . After straightforward calculations, we obtain:

$$\Gamma_l = l! \sum_{i=0}^{\infty} \frac{A^i h^{i+l+1}}{(i+l+1)!} \tag{6}$$

It is thus easy to see that, due to the term  $\gamma_2$ ,  $P(\mathbf{x}_k)$  in (5) is a polynomial of degree 4 in  $\mathbf{x}_k$ . The equation (5) can be readily used as a scheme specialized for multi-affine systems of degree 2.

**Convergence.** A bound on the error in our approximation is given in the following theorem.

**Theorem 1.** *Let  $\bar{\mathbf{x}}(t_{k+1})$  be the approximate solution at time  $t_{k+1}$  (computed by (4)) and  $\mathbf{x}(\cdot)$  be the corresponding exact solution such that  $\bar{\mathbf{x}}(t_k) = \mathbf{x}(t_k)$ . Then, a bound on the local error is given by:  $\|\bar{\mathbf{x}}(t_{k+1}) - \mathbf{x}(t_{k+1})\| = \mathcal{O}(h^3)$ .*

The proof of this result is presented in Appendix. This theorem shows that the equation (4) is a *second order scheme*. In addition, we can show that the global error is also convergent. As one can see from the proof, the error bound depends on the Lipschitz constant of the non-linear function  $f$ . So now we can see the interest in separating the linear part since the Lipschitz constant of  $f$  is smaller than that of  $g$ .

**Higher order integration schemes.** Note that we have used an approximation of the exact solution  $\mathbf{x}(t_k + \tau)$  by its first order Taylor expansion around  $t_k$ . To obtain better convergence orders, we can use higher order expansions which results in integration schemes involving high order derivatives of  $f(\mathbf{x})$ . The derivation of such schemes is similar to the above development, but the degree of the resulting integration map  $P(\mathbf{x}_k)$  can be higher. In the other direction, if we use a simpler approximation  $\alpha(t_k + \tau) = \mathbf{x}_k$  for all  $\tau \in [t_k, t_{k+1})$ , then  $Q(\mathbf{x}_k) = \Gamma_0 f(\mathbf{x}_k)$  and we obtain the classic Euler scheme for the non-linear part. The advantage of this scheme is that the resulting polynomial  $Q(\mathbf{x}_k)$  has the same degree as  $f(\mathbf{x})$ . As we shall see later, the degree of the integration map is one of the factors determining the complexity of the reachability algorithm. It remains to compute the polynomial map  $Q(\mathbf{x}_k)$ , the problem we tackle in the next section.

### 3 Computing Polynomial Maps

The problem we are interested in can be formally stated as follows. Given a polynomial map  $\pi : \mathbb{R}^n \rightarrow \mathbb{R}^n$  of total degree  $d$  and a bounded set  $X \subset \mathbb{R}^n$ , we want to compute the image  $\pi(X)$  defined as:  $\pi(X) = \{\pi(\mathbf{x}) \mid \mathbf{x} \in X\}$ . We shall focus on the case where  $X$  is a simplex in  $\mathbb{R}^n$ .

#### 3.1 Bézier Simplices

To determine the image of a simplex by a polynomial map, we use the results on *Bézier simplices* [17]. We need to introduce first some notation.

A multi-index  $\mathbf{i} = (i[1], \dots, i[n+1])$  is a vector of  $(n+1)$  non-negative integers. We define the norm of  $\mathbf{i}$  by  $\|\mathbf{i}\| = \sum_{j=1}^{n+1} i[j]$  and let  $\mathcal{I}_n^d$  denote the set of all multi-indices  $\mathbf{i} = (i[1], \dots, i[n+1])$  with  $\|\mathbf{i}\| = d$ . We define two special multi-indices:  $\mathbf{e}_j$  is a multi-index that has all the components equal to 0 except for the  $j^{th}$  component which is equal to 1, and  $\mathbf{o}$  is a multi-index that has all the components equal to 0. We call  $\mathbf{o}$  the zero multi-index.

Let  $\Delta$  be a full-dimensional simplex in  $\mathbb{R}^n$  with vertices  $\{\mathbf{v}_1, \dots, \mathbf{v}_{n+1}\}$ . Given a point  $\mathbf{x} \in \Delta$ , let  $\lambda(\mathbf{x}) = (\lambda_1(\mathbf{x}), \dots, \lambda_{n+1}(\mathbf{x}))$  be the function that gives the barycentric coordinates of  $\mathbf{x}$  with respect to the vertices of  $\Delta$ , that is,  $\mathbf{x} = \sum_{j=1}^{n+1} \lambda_j(\mathbf{x})\mathbf{v}_j$  and  $\sum_{j=1}^{n+1} \lambda_j(\mathbf{x}) = 1$ . A *Bézier simplex* of degree  $d$  of the form  $\pi : \mathbb{R}^n \rightarrow \mathbb{R}^n$  is defined as<sup>2</sup>:

$$\pi(\mathbf{x}) = \sum_{\|\mathbf{i}\|=d} \mathbf{b}_i B_i^d(\lambda_1(\mathbf{x}), \dots, \lambda_{n+1}(\mathbf{x})) \tag{7}$$

where for a given multi-index  $\mathbf{i}$ ,  $\mathbf{b}_i$  is a vector in  $\mathbb{R}^n$  and  $B_i^d : \mathbb{R}^n \rightarrow \mathbb{R}$  is a *Bernstein polynomial* of degree  $d$  defined as:

$$B_i^d(y_1, \dots, y_{n+1}) = \binom{d}{\mathbf{i}} y_1^{i[1]} y_2^{i[2]} \dots y_{n+1}^{i[n+1]} \tag{8}$$

with the multimomial coefficient  $\binom{d}{\mathbf{i}} = \frac{d!}{i[1]! i[2]! \dots i[n+1]!}$ . In the above formula (7), each vector  $\mathbf{b}_i$  is called a *Bézier control point* and the set of all such  $\mathbf{b}_i$  form the *Bézier control net* of  $\pi$  with respect to  $\Delta$ .

Any polynomial can be written in form of a Bézier simplex, as in formula (7). This form is a popular way to write polynomials in computer aided geometric design (see [17] and references therein). The following properties of Bernstein polynomials are well-known. The Bernstein polynomials form a partition of unity, that is,  $\sum_{\|\mathbf{i}\|=d} B_i^d(y_1, \dots, y_{n+1}) = 1$ , and they are non-negative, that is,  $B_i^d(y_1, \dots, y_{n+1}) \geq 0$  for all  $0 \leq y_1, \dots, y_{n+1} \leq 1$ . These properties of Bernstein polynomials imply the following *shape properties* of Bézier simplices, which we shall use for reachability computation purposes.

---

<sup>2</sup> The definition holds for more general polynomials of the form  $\pi : \mathbb{R}^n \rightarrow \mathbb{R}^m$ .

**Lemma 1.** *Given an arbitrary point  $\mathbf{x} \in \Delta$ ,*

1. **[Convex hull property]** *the point  $\pi(\mathbf{x})$  lies inside the convex hull of the control net, that is  $\pi(\mathbf{x}) \in \text{conv}\{\mathbf{b}_i \mid i \in \mathcal{I}_n^d\}$ .*
2. **[End-point interpolation property]**  *$\pi$  interpolates the control net at the corner control points specified by  $\mathbf{b}_{de_k}$  for all  $k \in \{1, \dots, n + 1\}$ .*

Note that the number of multi-indices in  $\mathcal{I}_k^d$  is  $\binom{d+n}{n}$ ; therefore, the number of points  $\mathbf{b}_i$  is exactly  $\binom{d+n}{n} = \frac{(d+n)!}{d!n!}$ . We denote this number by  $\beta(n, d)$ .

These shape properties can be used to approximate polynomial maps. Indeed, the *convex hull property* in Lemma 1 shows that one can over-approximate  $\pi(\Delta)$  by taking the convex hull of the Bézier control net of  $\pi$  with respect to  $\Delta$ . In addition, this *over-approximation is tight* due to the above *end-point interpolation property*. In the rest of this section we focus on the problem of computing the Bézier control net of the polynomial  $\pi$ . To avoid confusion, it is worthy to emphasize that for reachability computation purposes, we are dealing with the systems whose vector fields are given in monomial form (i.e. sums of monomials), hence the integration map is also defined in this form. To compute the control points of a polynomial given in monomial forms, we shall exploit the techniques for approximating and designing polynomial curves and surfaces. However, it is important to mention that most of such existing tools deal with univariate or bivariate polynomials (often expressed in terms of control points), their application to solve our problem requires an adaptation to multivariate polynomials as well as geometric manipulation in general dimension.

### 3.2 Computing the Bézier Control Net

Our goal is to obtain the Bézier control net of a polynomial  $\pi$  given in monomial form. By the definition (7), the most natural approach is to solve the following interpolation problem. Let  $S$  be a set of  $\beta(n, d)$  points in  $\Delta$ . For each  $\mathbf{x} \in S$ , we evaluate  $\pi(\mathbf{x})$  and use (7) to obtain a system of linear equations with the coordinates of the Bézier control points  $\mathbf{b}_i$  as unknown variables. One can choose the set  $S$  such that the unique solution to these linear equations exists [18]. Although this method is conceptually simple, it may require solving a large linear system<sup>3</sup> (which is of size  $n * \beta(n, d)$ ). We shall use a more efficient approach based on the blossoming principle, which is summarized in the following theorem. A thorough description of this principle and its various applications can be found in [19, 20].

**Theorem 2 (Blossoming principle).** *For any polynomial  $\pi : \mathbb{R}^n \rightarrow \mathbb{R}^n$  of degree  $d$ , there is a unique symmetric  $d$ -affine map  $p : (\mathbb{R}^n)^d \rightarrow \mathbb{R}^n$  such that for all  $\mathbf{x} \in \mathbb{R}^n$   $p(\mathbf{x}, \dots, \mathbf{x}) = \pi(\mathbf{x})$ . The map  $p$  is called the blossom or the polar form of  $\pi$ .*

---

<sup>3</sup> The Gaussian elimination algorithm to solve a linear system of size  $m \times m$  has the time complexity  $O(m^3)$ .

We recall that a map  $q(\mathbf{x}_1, \dots, \mathbf{x}_d)$  is called *d-affine* if it is affine when all but one of its arguments are kept fixed; it is said to be symmetric if its value does not depend on the ordering of the arguments, that is, for any permutation  $(\mathbf{y}_1, \dots, \mathbf{y}_d)$  of  $(\mathbf{x}_1, \dots, \mathbf{x}_d)$  we have  $q(\mathbf{y}_1, \dots, \mathbf{y}_d) = q(\mathbf{x}_1, \dots, \mathbf{x}_d)$ . Given a polynomial  $\pi$ , the connection between its Bézier control net relative to a simplex  $\Delta$  and its blossom  $p$  is described by the following lemma.

**Lemma 2.** For all  $\mathbf{i} \in \mathcal{I}_n^d$ ,  $\mathbf{b}_i = p(\underbrace{\mathbf{v}_1, \dots, \mathbf{v}_1}_{\mathbf{i}[1]}, \underbrace{\mathbf{v}_2, \dots, \mathbf{v}_2}_{\mathbf{i}[2]}, \dots, \underbrace{\mathbf{v}_{n+1}, \dots, \mathbf{v}_{n+1}}_{\mathbf{i}[n+1]})$

where  $\{\mathbf{v}_1, \dots, \mathbf{v}_{n+1}\}$  are the vertices of  $\Delta$ .

This fact is also well-known [19], and we present its proof in Appendix, which can facilitate understanding the subsequent development.

**Computing the blossom.** We have seen that the Bézier control points can be computed by evaluating the blossom values at some particular points shown in Lemma 2. To compute them, we first derive an analytic expression of the polar form and then show how to compute this expression efficiently. We do so by extending the results for bivariate polynomial surfaces [21] to multivariate polynomials.

Before proceeding, we mention that the problem of computing the Bézier control net can be formulated as a problem of changing from the monomial basis to the Bézier basis, which can be solved using the algorithms proposed in [22, 23]. These algorithms also make use of the blossoming principle. The idea is to express the coordinates of the new basis vectors in the old basis, and then apply the transformation matrix to the old coefficients. However, when the polynomial representation is “sparse”, that is it contains many zero coefficients, this sparsity is not exploited. The method discussed in the following deals better with such sparsity since it considers only the monomials with non-null coefficients. More precisely, by “sparse polynomial representations” we mean those where the number of monomials (with non-null coefficients) is much smaller than the number of all combinations of coordinate variables up to degree  $d$ . The sparse case indeed happens in many practical applications we have encountered.

Let us now show how to compute the blossom of monomials which are products of only two variables, such as  $\mathbf{x}[i]^h \mathbf{x}[j]^k$ . Similar treatment can be used for monomials involving more variables, but due to the length of the involved formulas we do not detail it here. On the other hand, using linearity, we can obtain the blossom of any polynomial expressed as a sum of monomials.

The blossom of degree  $d$  of the monomial  $(\mathbf{x}[i])^h (\mathbf{x}[j])^k$  is given by:

$$p_{h,k}^d(\mathbf{u}_1, \mathbf{u}_2, \dots, \mathbf{u}_d) = \frac{1}{\binom{d}{h} \binom{d-h}{k}} \sum_{\substack{I \cup J \subset \{1, \dots, d\}, \\ |I| = h, |J| = k, I \cap J = \emptyset}} \prod_{r \in I} \mathbf{u}_r[i] \prod_{s \in J} \mathbf{u}_s[j].$$

To prove this, it suffices to check that the right hand side is a symmetric multi-affine function, and moreover  $p_{h,k}^d(\mathbf{u}, \mathbf{u}, \dots, \mathbf{u}) = (\mathbf{u}[i])^h (\mathbf{u}[j])^k$ .  $\square$

To compute the blossom values using the above expression, we make use of a recurrence equation on  $p$ , as proposed in [21]. We first denote

$$\sigma_{h,k}^d = \frac{1}{\binom{d}{h} \binom{d-h}{k}} p_{h,k}^d(\mathbf{u}_1, \mathbf{u}_2, \dots, \mathbf{u}_d).$$

The function  $\sigma$  is symmetric and has the following interpretation: this function is computed by choosing  $h$   $i^{th}$  coordinates of the argument points and  $k$   $j^{th}$  coordinates and forming their product, then summing these products over all possible choices. We can thus derive the following recurrence formula:

$$\begin{cases} \sigma_{h,k}^d = \sigma_{h,k}^{d-1} + \mathbf{u}_d[i] \sigma_{h-1,k}^{d-1} + \mathbf{u}_d[j] \sigma_{h,k-1}^{d-1} & \text{if } h, k \geq 0 \text{ and } h+k \geq 1, \\ \sigma_{0,0}^d = 0 \end{cases} \quad (9)$$

This means that to compute the required blossom value  $p_{h,k}^d(\mathbf{u}_1, \mathbf{u}_2, \dots, \mathbf{u}_d)$  we compute all the intermediate values  $p_{h',k'}^{d'}$  with  $d' \leq d$ ,  $h' + k' \leq d'$ . This computation can be done in time  $O(d^3)$ .

### 3.3 Approximation Error and Subdivision

We proceed to estimate an error bound for the approximation of the polynomial map  $\pi$  by its the Bézier control points.

**Theorem 3.** *For each Bézier control point  $\mathbf{b}_i$  there exists a point  $\mathbf{y} \in \pi(\Delta)$  such that  $\|\mathbf{b}_i - \mathbf{y}\| \leq K\rho^2$  where  $\rho$  be the maximal side length of  $\Delta$  and  $K$  is some constant not depending on  $\Delta$ .*

The proof of this theorem can be found in Appendix.

Consequently, when the simplicial domain  $\Delta$  is large, to achieve the desired accuracy we may need to subdivide it into smaller simplices. This subdivision creates new Bézier bases and therefore new control points. However, due to the properties of multi-affine maps, one can compute the new control nets in a clever way which reuses the computations performed for the original simplex. Suppose that we want to partition the simplex  $\Delta$  by adding a point  $\mathbf{x} \in \Delta$  and forming  $(n+1)$  new smaller simplices. Then, we can use de Catesljau algorithm [24, 17] to compute the value of the polynomial  $\pi$  at  $\mathbf{x}$ . It turns out that this computation also produces the control net for the new simplices. Note that this algorithm can only be applied when the Bézier control points of the polynomial are known.

We denote  $\mathbf{b}_i^l = p(\underbrace{\mathbf{v}_1, \dots, \mathbf{v}_1}_{i[1]}, \dots, \underbrace{\mathbf{v}_{n+1}, \dots, \mathbf{v}_{n+1}}_{i[n+1]}, \underbrace{\mathbf{x}_1, \dots, \mathbf{x}_l}_l)$  with  $i[1] + \dots + i[n+1] + l = d$ . Since  $p$  is symmetric and multi-affine, we have:

$$\mathbf{b}_i^l = \lambda_1(\mathbf{x}_l) \mathbf{b}_{i+\mathbf{e}_1}^{l-1} + \dots + \lambda_n(\mathbf{x}_l) \mathbf{b}_{i+\mathbf{e}_n}^{l-1} \quad (10)$$

Note that  $\mathbf{b}_\mathbf{o}^n = p(\mathbf{x}_1, \dots, \mathbf{x}_n)$  where  $\mathbf{o}$  is the zero multi-index. In addition, with  $l = 0$ ,  $\mathbf{b}_i^0$  are exactly the Bézier control points of the polynomial. Therefore, by running the above recursion starting from  $l = 0$  until  $l = n$  we obtain the blossom value at  $(\mathbf{x}_1, \dots, \mathbf{x}_n)$ . If all the argument points of the blossom are equal



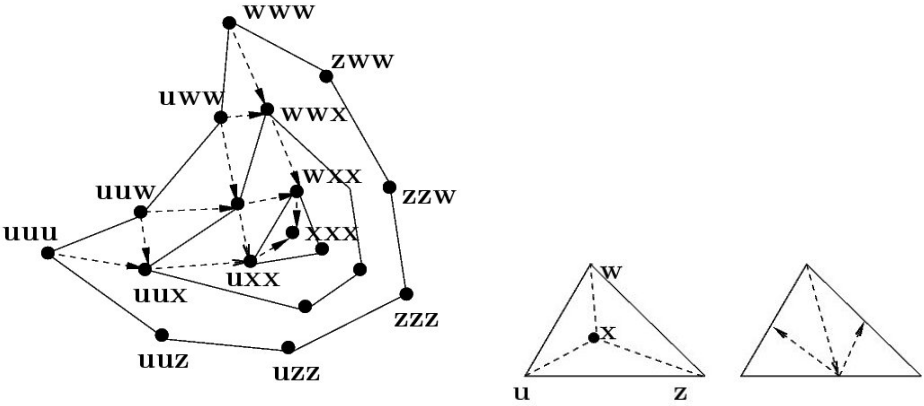


Fig. 1. Subdividing a Bézier control net

to  $\mathbf{x}$ , the result of the algorithm is  $\pi(\mathbf{x})$ . The de Catesljau algorithm is illustrated with a 2-dimensional example in Figure 1 where each node is annotated with the arguments of the blossom to evaluate. The nodes on the outermost layer correspond to the control points for the original triangle  $\mathbf{u}\mathbf{z}\mathbf{w}$ . The incoming arrows of  $\mathbf{u}\mathbf{u}\mathbf{x}$  show that the blossom value at this point is computed from the blossom values at  $\mathbf{u}\mathbf{u}\mathbf{u}$  and  $\mathbf{u}\mathbf{u}\mathbf{w}$ . As mentioned earlier, we can see that the computation of  $\pi(\mathbf{x})$  indeed produces the Bézier control points for the sub-simplices. Figure 1 shows the values  $p(\underbrace{\mathbf{u}, \dots, \mathbf{u}}_{i[1]}, \underbrace{\mathbf{x}, \dots, \mathbf{x}}_{i[2]}, \underbrace{\mathbf{w}, \dots, \mathbf{w}}_{i[3]})$  which are the

Bézier control points for the triangle  $\mathbf{u}\mathbf{x}\mathbf{w}$ .

One important remark is that the subdivision at the center of the simplex does not reduce the maximal side length of the simplices. By Theorem 3 this means that the convergence of the Bézier control net towards the polynomial is not guaranteed. However, one can repeat the bisection at the mid-point of the longest edge, as shown in Figure 1 to achieve the desired accuracy. More generally, the subdivision of a simplex can be defined as follows. For each barycentric coordinate  $\lambda_i(\mathbf{x}) > 0$  of a point  $\mathbf{x} \in \Delta$  we define a simplex  $\Delta_i$  obtained from  $\Delta$  by replacing the vertex  $\mathbf{v}_i$  with  $\mathbf{x}$ . Hence, when the point  $\mathbf{x}$  is the mid-point of an edge we obtain a bisection. It was proved in [25] that using the bisection at the mid-point of the longest edge, after  $n$  steps (where  $n$  is the dimension of the simplex) the simplex diameter is reduced at least by  $\sqrt{3}/2$  times. In two dimensions, another method of subdivision via all the mid-points of the edges was discussed in [21]. This method is however more complex to implement for dimensions higher than 2.

### 4 Reachability Algorithm

Let us summarize our development so far. In Section 2, we presented a scheme to approximate the successor in one time step by applying a polynomial, called

the integration map, to the current state. We then showed in Section 3 how to over-approximate the image of a simplex by a polynomial map using the Bézier control net. The result of this approximation is in general a polyhedron.

We are now ready to describe our reachability algorithm for polynomial systems. In Algorithm 1,  $X_0$  is the initial set which is assumed to be a convex polyhedron in  $\mathbb{R}^n$ , each  $R_k$  is a set of convex polyhedra. The function *Bez* over-approximates the image of a simplex  $\Delta$  by the integration map  $P$ , using the method presented in Section 3. The goal of the function *triangulation* is to triangulate a set of convex polyhedra and return the set of all simplices of the triangulation. To do so, we collect all the vertices of the polyhedra and compute a triangulation of this set. We then exclude all the simplices in the triangulation whose interior does not intersect with  $R_k$ . Let us briefly discuss the precision of

---

**Algorithm 1.** Reachable set computation

---

```

 $R_0 = \{X_0\}, k = 0$ 
repeat
   $S_\Delta = \text{triangulation}(R_k)$ 
   $C = \emptyset$ 
  for all  $\Delta \in S_\Delta$  do
     $C = C \cup \text{Bez}(\Delta)$ 
  end for
   $R_{k+1} = C$ 
   $k = k + 1$ 
until  $R_{k+1} = R_k$ 

```

---

the algorithm. We suppose that  $\rho$  is the maximal size of the simplices that are produced by the function *triangulation* and  $h$  is the integration time step. If the integration map  $P$  can be exactly computed, using Theorem 1, the integration error is  $\mathcal{O}(h^3)$ . In addition, Theorem 3 shows that our approximation of the integration map  $P$  induces an error  $\mathcal{O}(\rho^2)$ . By the triangle inequality, the total error in each iteration of Algorithm 1 is bounded by  $(\mathcal{O}(h^3) + \mathcal{O}(\rho^2))$ . Therefore, by choosing appropriate values  $\rho$  in function of  $h$ , we can guarantee a bound  $\mathcal{O}(h^3)$  on the local error and thus the order 2 of Algorithm 1.

We now discuss some computation issues. The first remark is that the total number of the Bézier control points is  $\beta(n, d)$ , but the actual number of vertices of their convex hull (that is,  $\text{Bez}(\Delta)$ ) is often much smaller, depending on the geometric structure of the polynomial map  $P$ . On the other hand, in order to speed up the computation (at the price of less precise results), one can approximate  $C$  by its convex hull or even by a simplex. Algorithms for doing so have been developed and some algorithms can compute a minimal volume enclosing simplex (such as, [26, 27]).

Let us now briefly discuss the relation between our new algorithm and the reachability algorithm based on hybridization, proposed in [15]. The latter first approximates the (general) non-linear dynamics by a piecewise linear dynamics, using a simplicial decomposition of the state space. Hence, for the approximate

system, one can indeed compute the reachable set of each linear dynamics more accurately. However, the treatment of discrete transitions (i.e. the dynamics changes) makes the overall computation very expensive due to the geometric complexity of the intersection between the reachable set and the switching hyperplanes. In the algorithm of this paper, the one-step computation for polynomial systems is in general more costly than that for linear systems, but discrete transitions are avoided. Nevertheless, more experimentation is needed to draw conclusions about the advantages and inconvenients of these two approaches.

## 5 Application to a Biological System

We have implemented Algorithm 1 and applied it to a well-known biological system. The initial motivation of our study of polynomial systems come from the interest in applying hybrid systems techniques to biological systems. Indeed, the continuous dynamics of many such systems can be described using multi-affine or more generally polynomial differential equations. We have experimented the implementation of our algorithm on two simplified models of gene transcription control in the bacteria *Vibrio Fisheri*. The reader is referred to the papers [28, 29] for a detailed description of the models and the related gene control problems. The first model corresponds to one mode of a simplified hybrid system where the continuous dynamics is described by the following multi-affine system:

$$\begin{cases} \dot{x}_1 = k_2 x_2 - k_1 x_1 x_3 + u_1 \\ \dot{x}_2 = k_1 x_1 x_3 - k_2 x_2 \\ \dot{x}_3 = k_2 x_2 - k_1 x_1 x_3 - n x_3 + n u_2 \end{cases} \quad (11)$$

The state variables  $\mathbf{x} = (x_1, x_2, x_3)$  represent the cellular concentrations of different species, and the parameters  $k_1, k_2, n$  are the binding, dissociation and diffusion constants. The variables  $u_1$  and  $u_2$  are control variables, which respectively represent the plasmid and external source of autoinducer. In [29] the following control law for steering all the states in the rectangle  $[1, 2] \times [1, 2] \times [1, 2]$

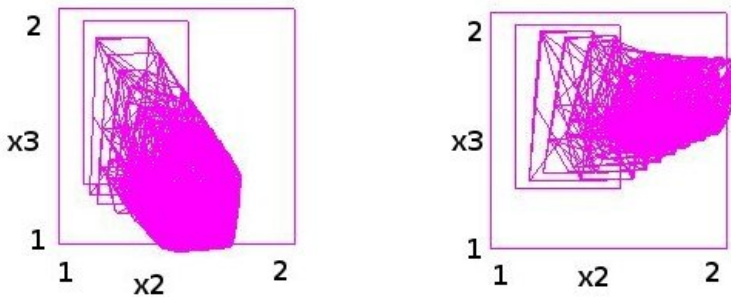


**Fig. 2.** Reachable sets: with  $u_1 = u_2 = 0$  (left) and with the specified control law (right). The control law indeed drives the system to the face  $x_2 = 2$ .

to the face  $x_2 = 2$  was proposed:  $u_1(\mathbf{x}) = -10(x_2 + x_1(-1 + 3) - 4x_3)$  and  $u_2(\mathbf{x}) = x_1(3 + x_2(-1 + x_3)) - (-2 + x_2)x_3$ . This control objective corresponds to the activation of some genes in the system. We consider two cases: with no control (i.e.  $u_1 = u_2 = 0$ ) and with the above control law. Figure 2 shows the projection on  $x_2$  and  $x_3$  of the reachable sets obtained using our algorithm for polynomial systems. In [16] we have already treated this model using an abstraction method based on projection. This method approximates the multi-affine system by a lower dimensional bilinear system. Comparing with the result presented in [16], one can see that our new algorithm for polynomial systems is more accurate, and in addition we have observed that it is also more time-efficient.

The second model is taken from [28]. It is a hybrid model<sup>4</sup> with two modes and one additional continuous variable  $x_4$ . The continuous dynamics is  $\dot{\mathbf{x}} = A\mathbf{x} + g(\mathbf{x}) + b_{ij}$  where  $b_{01}$  and  $b_{10}$  correspond respectively to the non-luminescent and luminescent modes, and

$$A = \begin{pmatrix} \frac{-1}{H_{sp}} & 0 & 0 & r_{Co} \\ 0 & 0 & 0 & \frac{-1}{H_{sp}} - r_{Co} \\ 0 & x_0 r_{AII} & \frac{-1}{H_{AI}} & x_0 r_{Co} \\ 0 & \frac{-1}{H_{sp}} & 0 & 0 \end{pmatrix}; g(\mathbf{x}) = \begin{pmatrix} -1 \\ 1 \\ -x_0 \\ 0 \end{pmatrix} r_{AIR} x_1 x_3$$

We are interested in the question of how to determine the sets of states from which the system can reach the luminescent equilibrium. The condition for switching between the two modes is  $x_2 = x_{2sw}$ . This problem was also previously studied in [28] using the tool  $\mathbf{d}/\mathbf{dt}$ . However, in [28] the multi-affine dynamics was approximated by a 3-dimensional linear system, assuming that  $x_1$  remains constant. Using our new algorithm for polynomial systems, we can now handle the non-linearity in the dynamics. To deal with the discrete dynamics of the model, it suffices to implement some Boolean operations over the reachable set by the continuous dynamics, which are represented in form of convex polyhedra. Concerning qualitative behavior, the result obtained for the 4-dimensional multi-affine model is compatible with the result for the linear approximate model in [28], that is, from the non-luminescent mode the system can reach the guard to switch to the luminescent mode and then converge to the equilibrium. However, the new result obtained for the 4-dimensional model shows a larger set of states that can reach the equilibrium. This can be explained by the fact that in this model the variable  $x_1$  is not kept constant and can evolve in time.

## 6 Concluding Remarks

In this paper, we presented a new approach to approximate reachability analysis of polynomial systems by combining the ideas from numerical integration and techniques from computer aided geometric design. The reachability algorithm we proposed is of order 2, and these results can be straightforwardly applied to safety verification of hybrid systems. This work opens interesting directions to

<sup>4</sup> The numbering of variables is different from that in [28].

explore. Indeed, different tools from geometric modeling (such as, splines) could be exploited to approximate polynomial maps more efficiently. In addition, we plan to do more experimentation on other case studies, such as a model of metabolic mechanism of a plant.

## References

1. Alur, R., Henzinger, T., Lafferriere, G., Pappas, G.: Discrete abstractions of hybrid systems. *Proc. of the IEEE* (2000)
2. Greenstreet, M., Mitchell, I.: Integrating projections. In Henzinger, T., Sastry, S., eds.: *Hybrid Systems: Computation and Control*. LNCS 1386, Springer (1998) 159–1740
3. Dang, T., Maler, O.: Reachability analysis via face lifting. In Henzinger, T., Sastry, S., eds.: *Hybrid Systems: Computation and Control*. LNCS 1386, Springer (1998) 96–109
4. Chutinan, A., Krogh, B.: Verification of polyhedral invariant hybrid automata using polygonal flow pipe approximations. In Vaandrager, F., van Schuppen, J., eds.: *Hybrid Systems: Computation and Control*. LNCS 1569, Springer (1999) 76–90
5. Kurzanski, A., Varaiya, P.: Ellipsoidal techniques for reachability analysis. In Krogh, B., Lynch, N., eds.: *Hybrid Systems: Computation and Control*. LNCS 1790, Springer (2000) 202–214
6. Asarin, E., Bournez, O., Dang, T., Maler, O.: Approximate reachability analysis of piecewise-linear dynamical systems. In Krogh, B., Lynch, N., eds.: *Hybrid Systems: Computation and Control*. LNCS 1790, Springer (2000) 20–31
7. Tomlin, C., Mitchell, I., Bayen, A., Oishi, M.: Computational techniques for the verification of hybrid systems. *Proceedings of the IEEE* **91**(7) (2003) 986–1001
8. Mitchell, I.M., Templeton, J.A.: A toolbox of Hamilton-Jacobi solvers for analysis of nondeterministic continuous and hybrid systems. In: *Hybrid Systems: Computation and Control*. LNCS, Springer (2005, to appear)
9. Girard, A.: Reachability of uncertain linear systems using zonotopes. In: *Hybrid Systems : Computation and Control*. LNCS 3414, Springer (2005) 291–305
10. Prajna, S., Jadbabaie, A.: Safety verification of hybrid systems using barrier certificates. In Alur, R., Pappas, G.J., eds.: *Hybrid Systems: Computation and Control*. LNCS 2993, Springer (2004) 477–492
11. Tiwari, A., Khanna, G.: Nonlinear systems: Approximating reach sets. In: *Hybrid Systems: Computation and Control*. LNCS 2993, Springer (2004) 600–614
12. Tiwari, A., Khanna, G.: Series of abstractions for hybrid automata. In Tomlin, C., Greenstreet, M., eds.: *Hybrid Systems: Computation and Control*. LNCS 2289, Springer (2002) 465–478
13. Alur, R., Dang, T., Ivancic, F.: Reachability analysis via predicate abstraction. In Greenstreet, M., Tomlin, C., eds.: *Hybrid Systems: Computation and Control*. LNCS 2289, Springer (2002)
14. Clarke, E.M., Fehnker, A., Han, Z., Krogh, B.H., Ouaknine, J., Stursberg, O., Theobald, M.: Abstraction and counterexample-guided refinement in model checking of hybrid systems. *Int. J. Found. Comput. Sci.* **14**(4) (2003) 583–604
15. Asarin, E., Dang, T., Girard, A.: Reachability analysis of nonlinear systems using conservative approximation. In Maler, O., Pnueli, A., eds.: *Hybrid Systems: Computation and Control*. LNCS 2623, Springer (2003) 20–35

16. Asarin, E., Dang, T.: Abstraction by projection. In Alur, R., Pappas, G., eds.: Hybrid Systems: Computation and Control. LNCS 2993, Springer (2004) 32–47
17. Farin, G.: Curves and Surfaces for Computer Aided Geometric Design. Academic Press (1990)
18. Davyrov, O., M.Sommer, H.Strauss: On almost interpolation by multivariate splines. In G.Nürnbergger, J., G.Walz, eds.: Multivariate Approximation and Splines, ISNM, Birkhäuser (1997) 45–58
19. Ramshaw, L.: Blossoms are polar forms. Computer Aided Geometric Design **6** (1989) 323–358
20. Seidel, H.P.: Polar forms and triangular B-spline surfaces. In: Blossoming: The New Polar-Form Approach to Spline Curves and Surfaces, SIGGRAPH '91 Course Notes 26, ACM SIGGRAPH. (1991) 8.1–8.52
21. Gallier, J.: Curves and surfaces in geometric modeling: theory and algorithms. Series In Computer Graphics and Geometric Modeling. Morgan Kaufmann (1999)
22. DeRose, T., Goldman, R., Hagen, H., Mann, S.: Functional composition via blossoming. ACM Transactions on Graphics **12**(2) (April 1993)
23. Lodha, S., Goldman, R.: Change of basis algorithms for surfaces in cagd. Computer Aided Geometric Design **12** (1995) 801–824
24. de Casteljau, P.: Formes à pôles. Hermes, Paris (1985)
25. Rivara, M.C.: Mesh refinement process based on the generalized bisection of simplices. SIAM Journal on Numerical Analysis **21** (1984) 604–613
26. Vegter, G., Yap, C.: Minimal circumscribing simplices. In: Proc. of the 3rd Canadian Conference on Computational Geometry, Vancouver, Canada. (1991) 58–61
27. Fuhrmann, D.R.: A simplex shrink-wrap algorithm. In: Proceedings of SPIE, AeroSense (1999)
28. Belta, C., Schug, J., Dang, T., Kumar, V., Pappas, G., Rubin, H., Dunlap, P.: Stability and reachability analysis of a hybrid model of luminescence in the marine bacterium *vibrio fisheri*. In: Proc. of CDC. (2001)
29. Belta, C., Habets, L.C.G.J.M., Kumar, V.: Control of multi-affine systems on rectangles with an application to gene transcription control. In: Proc. of CDC. (2003)

**Proof of Theorem 1.** From (3) and (4), the local error can be written as:

$$\mathbf{x}(t_k + \tau) - \bar{\mathbf{x}}(t_k + \tau) = \int_0^h e^{A(h-\tau)} [f(\mathbf{x}(t_k + \tau)) - f(\boldsymbol{\alpha}(t_k + \tau))] d\tau.$$

On the other hand, due to the Taylor expansion, we have  $\|\mathbf{x}(t_k + \tau) - \boldsymbol{\alpha}(t_k + \tau)\| \leq M\tau^2$  where  $M$  is some constant. We then have  $\|f(\mathbf{x}(t_k + \tau)) - f(\boldsymbol{\alpha}(t_k + \tau))\| \leq LM\tau^2$  where  $L$  is the Lipschitz constant of  $f$ . Using the expression (6), we have  $\Gamma_2 = \int_0^h e^{A(h-\tau)} \tau^2 d\tau = \frac{A^3}{3!} h^3 + \mathcal{O}(h^4)$ , it then follows that

$$\|\mathbf{x}(t_k + \tau) - \bar{\mathbf{x}}(t_k + \tau)\| = \mathcal{O}(h^3).$$

This completes the proof of the theorem. □

**Proof of Lemma 2.** We consider  $p(\mathbf{x}_1, \mathbf{x}_2, \dots, \mathbf{x}_d)$  where each argument  $\mathbf{x}_j$  can be expressed using the barycentric coordinates as:  $\mathbf{x}_j = \lambda_1(\mathbf{x}_j)\mathbf{v}_1 + \dots +$

$\lambda_{n+1}(\mathbf{x}_j)\mathbf{v}_{n+1}$ . Due to the property of multi-affine maps, replacing the first argument  $\mathbf{x}_1$  with its barycentric coordinates, we have:

$$p(\mathbf{x}_1, \mathbf{x}_2, \dots, \mathbf{x}_d) = \lambda_1(\mathbf{x}_1)p(\mathbf{v}_1, \mathbf{x}_2, \dots, \mathbf{x}_{n+1}) + \dots + \lambda_{n+1}(\mathbf{x}_1)p(\mathbf{v}_{n+1}, \mathbf{x}_2, \dots, \mathbf{x}_{n+1}).$$

We then do the same with other arguments to obtain:

$$p(\mathbf{x}_1, \dots, \mathbf{x}_d) = \sum_{I \in \Xi} \prod_{k \in I_1} \lambda_1(\mathbf{x}_k) \dots \prod_{k \in I_{n+1}} \lambda_{n+1}(\mathbf{x}_k) p(\underbrace{\mathbf{v}_1, \dots, \mathbf{v}_1}_{\mathbf{i}[1]}, \dots, \underbrace{\mathbf{v}_{n+1}, \dots, \mathbf{v}_{n+1}}_{\mathbf{i}[n+1]}) \tag{12}$$

where  $\Xi$  is the set of all partitions of  $\{1, 2, \dots, d\}$  defined as follows. We say that  $I = \{I_k\}_{k=1,2,\dots,n+1}$  is a partition of  $\{1, 2, \dots, d\}$  iff all  $I_k$  are pairwise disjoint and  $\cup_{k \in \{1,\dots,n+1\}} I_k = \{1, 2, \dots, d\}$ . We write  $|I_k|$  to denote the cardinality of  $I_k$ . Then, by letting the arguments  $\mathbf{x}_i$  to be equal, it is not hard to see that the equation (12) becomes:

$$p(\mathbf{x}, \dots, \mathbf{x}) = \sum_{\|\mathbf{i}\|=d} \binom{d}{\mathbf{i}} \lambda_1^{\mathbf{i}[0]}(\mathbf{x}) \lambda_2^{\mathbf{i}[1]}(\mathbf{x}) \dots \lambda_n^{\mathbf{i}[n]}(\mathbf{x}) p(\underbrace{\mathbf{v}_1, \dots, \mathbf{v}_1}_{\mathbf{i}[1]}, \dots, \underbrace{\mathbf{v}_{n+1}, \dots, \mathbf{v}_{n+1}}_{\mathbf{i}[n+1]})$$

Comparing the above with the definition of Bézier simplices (7), it is easy to see that all the points  $p(\underbrace{\mathbf{v}_1, \dots, \mathbf{v}_1}_{\mathbf{i}[1]}, \dots, \underbrace{\mathbf{v}_{n+1}, \dots, \mathbf{v}_{n+1}}_{\mathbf{i}[n+1]})$  form the control net of a  $\pi$  whose polar form is  $p$ . □

**Proof of Theorem 3.** Given a multi-index  $\mathbf{i}$  with  $\|\mathbf{i}\| = d$ , we consider a point  $\mathbf{y} \in \Delta$  which is written as  $\mathbf{y} = \sum_{i \in \{1,\dots,n\}} \frac{\mathbf{i}[i]}{d} \mathbf{v}_i$ . We first observe that due to symmetry,  $p(\mathbf{x}, \mathbf{y}, \dots, \mathbf{y}) = p(\mathbf{y}, \mathbf{x}, \dots, \mathbf{y}) = \dots = p(\mathbf{y}, \mathbf{y}, \dots, \mathbf{x})$ . Let  $D$  denote the partial derivative of these functions at  $\mathbf{x} = \mathbf{y}$ . Using the Taylor expansion of  $p(\mathbf{x}_1, \mathbf{x}_2, \dots, \mathbf{x}_d)$  around  $(\mathbf{y}, \mathbf{y}, \dots, \mathbf{y})$ , we have:

$$\begin{aligned} \mathbf{b}_\mathbf{i} &= p(\underbrace{\mathbf{v}_1, \dots, \mathbf{v}_1}_{\mathbf{i}[1]}, \dots, \underbrace{\mathbf{v}_{n+1}, \dots, \mathbf{v}_{n+1}}_{\mathbf{i}[n+1]}) \\ &= p(\mathbf{y}, \mathbf{y}, \dots, \mathbf{y}) + \mathbf{i}[1]D(\mathbf{v}_1 - \mathbf{y}) + \dots + \mathbf{i}[n+1]D(\mathbf{v}_{n+1} - \mathbf{y}) + O(\rho^2) \end{aligned}$$

Note that  $\mathbf{i}[0](\mathbf{v}_0 - \mathbf{y}) + \dots + \mathbf{i}[n+1](\mathbf{v}_{n+1} - \mathbf{y}) = 0$ . It then follows that  $\mathbf{b}_\mathbf{i} = \pi(\mathbf{y}) + O(\rho^2)$ . This means that  $\|\mathbf{b}_\mathbf{i} - \pi(\mathbf{y})\|$  is indeed of order  $O(\rho^2)$ . □